Towards an improved prediction of concentrated antibody solution viscosity using the Huggins coefficient

DOI:
10.1016/j.jcis.2021.08.191

Document Version
Accepted author manuscript

Towards an improved prediction of concentrated antibody solution viscosity using the Huggins coefficient

Aisling Roche[a,f], Lorenzo Gentiluomo[b,c,e], Nicole Sibanda[a], Dierk Roessner[b], Wolfgang Friess[c], Steven P. Trainoff[d], Robin Curtis[a,*]

[a] *Manchester Institute of Biotechnology, University of Manchester, 131 Princess Street, School of Chemical Engineering and Analytical Science, Manchester M1 7DN,UK*
[b] *Wyatt Technology Europe GmbH, Hochstrasse 18, 56307 Dernbach, Germany 2*
[c] *Department of Pharmacy; Pharmaceutical Technology and Biopharmaceutics; Ludwig-Maximilians-Universität München, Butenandtstrasse 5, 81377 Munich, Germany*
[d] *Wyatt Technology Corporation, 6330 Hollister Ave, Goleta, CA 93117, United States*
[e] *Currently at: Coriolis Pharma, Fraunhoferstraße 18B, 82152 Munich, Germany*
[f] *Currently at: National Institute for Biological Standards and Control, South Mimms, Potters Bar, Herts EN6 3QG, UK*

Abstract

The viscosity of a monoclonal antibody solution must be monitored and controlled as it can adversely affect product processing, packaging and administration. Engineering low viscosity mAb formulations is challenging as prohibitive amounts of material are required for concentrated solution analysis, and it is difficult to predict viscosity from parameters obtained through low-volume, high-throughput measurements such as the interaction parameter, k_{D}, and the second osmotic virial coefficient, B_{22}. As a measure encompassing the effect of intermolecular interactions on dilute solution viscosity, the Huggins coefficient, k_{h}, is a promising candidate as a parameter measureable at low concentrations, but indicative of concentrated solution

*Corresponding Author
Email address: r.curtis@manchester.ac.uk (Robin Curtis)

viscosity. In this study, a differential viscometry technique is developed to measure the intrinsic viscosity, $[\eta]$, and the Huggins coefficient, k_{h}, of protein solutions. To understand the effect of colloidal protein-protein interactions on the viscosity of concentrated protein formulations, the viscometric parameters are compared to k_{D} and B_{22} of two mAbs, tuning the contributions of repulsive and attractive forces to the net protein-protein interaction by adjusting solution pH and ionic strength. We find a strong correlation between the concentrated protein solution viscosity and the k_{h} but this was not observed for the k_{D} or the b_{22}, which have been previously used as indicators of high concentration viscosity. Trends observed in $[\eta]$ and k_{h} values as a function of pH and ionic strength are rationalised in terms of protein-protein interactions.
Keywords: Monoclonal antibodies, Rheology, Protein-protein interactions, Huggins coefficient, Intrinsic viscosity

1. Introduction

Monoclonal antibodies are regularly formulated at high protein concentrations to meet drug potency requirements within the 1 mL injection volume limitations of subcutaneous administration[1,2]. High concentration protein formulations can result in unacceptably high viscosities over 30 cP, which cause difficulties in manufacturing, increased injection force demands, and pain during patient administration[1,3,4]. Next generation biologics such a bispecific antibodies and Fc-fusion proteins are also likely to have viscosities in the problematic range[5,6].

The concentrated solution viscosity of protein solutions is difficult to pre-

dict. Viscosity data of proteins has been shown to fit well to colloidal models such as the Krieger-Dougherty and Ross-Minton-Mooney models when parameters are allowed to vary freely, but the resulting parameters are often incongruous with independent measurements or theoretical calculations based on protein properties. Fitting the viscosity data of BSA solutions up to high concentrations using the Krieger-Dougherty model resulted in unrealistic maximum volume fraction values and intrinsic viscosities much higher than those measured in dilute solution[7,8]. The effective intrinsic viscosity values obtained from the fits of the Ross-Minton-Mooney model to mAb viscosity data[9,10,11] are often in excess of $10\,\mathrm{mL\,g^{-1}}$, however mAb solutions more commonly have an intrinsic viscosity of between 6 and $7\,\mathrm{mL\,g^{-1}}$ when measured in dilute solution[12,13,14,15]. Quantitatively predicting protein solution viscosity using colloidal models is therefore impractical as parameterising the models with independent dilute solution measurements requires substantial effort but rarely captures concentrated solution behaviour.

One reason colloidal hard-sphere rheological models do not accurately predict concentrated protein solution viscosity is that the models do not explicitly account for the effects of protein-protein interactions(PPI). An alternative approach for predicting concentrated solution viscosity is to seek correlations with dilute solution parameters reflecting PPI, such as the diffusion coefficient interaction parameter, k_D, or the second osmotic virial coefficient, B_{22}. In two studies comparing large datasets obtained for multiple mAbs in the same formulation, a negative k_D or B_{22}, denoting attractive PPI, was correlated with high sample viscosities[16,17]. When varying pH and ionic strength, a maximum in mAb viscosity is sometimes observed at pH conditions closest

to the protein isoelectric point at low ionic strength, which corresponds to the solution with the strongest protein-protein attractions[18,19]. The direct relationship between net PPI and the high concentration viscosity does not hold for other studies. Correlations between attractive k_D or B_{22} values and high concentration viscosities were weak, protein-specific or not observed in several investigations[19,14,20,18,10,20].

A key shortcoming of using k_D or B_{22} is that the parameters relate to an averaged protein-protein interaction, which does not reflect the orientational correlations between a pair of interacting proteins. As such, the measurements are not sensitive to anisotropic interactions that occur between many mAbs due to electrostatic attractions arising from surface charge heterogeneity and presence of non-polar surface patches[21,22,23,24,25]. At low protein concentrations, anisotropic interactions stabilize reversible oligomers, which further associate at high protein concentrations to form transient networks or clusters[26,22,10,9,27,28]. The cluster properties are key determininants of the viscosity. For some mAbs, the viscosity scales linearly with the cluster size[26], while other mAbs exhibit non-monotonic relationships between the viscosity and cluster size[10]. The contrasting behaviour has been rationalized in terms of cluster shapes and their effective volumes, which are determined by the valency of the mAb-mAb interactions[10,27,9,22,28]. Linear viscosity profiles with respect to cluster size are expected when clusters are more open, which occurs for low valancy interactions. On the other hand, higher valency interactions lead to more compact clusters which contribute less to the solution viscosity when compared against linear clusters of the same size.

The correlation of viscosity with dilute solution parameters fails because

the parameters do not uniquely determine the micro-structure of the concentrated solutions. However, properties measured at high protein concentration also do not exhibit a strong correlation with viscosity. No generalised correlations between the high concentration parameters, zero-q structure factor, $S_{\mathrm{q=0}}$ and zero-q hydrodynamic function, $H_{\mathrm{q=0}}$, and high concentration viscosity were found when multiple mAb systems in formulations varying in pH, ionic strength and excipient composition were compared[9,29]. On the other hand, a recent study has shown that the viscosity can be predicted from measurements of osmotic compressibility and mutual diffusion coefficients made up to high protein concentrations[30]. In that study, the thermodynamic measurements were used to parameterize a patchy colloidal model, which in turn, was used to estimate cluster size and volume as a function of protein concentration. The Mooney equation was used to calculate the viscosity by treating the clusters as polydisperse spheres. Further investigations are required to see if the approach can capture behaviour of other mAbs which display different patterns of cluster formation.

The search for a parameter which can be measured using minimal protein material, and which reliably correlates to the viscosity of the solution at high protein concentrations in physiological formulation conditions is ongoing. A dilute solution parameter that has the potential to correlate well with high protein concentration solution viscosity is the Huggins coefficient, k_{h}. The Huggins coefficient is derived from the linear concentration-dependence of the dilute solution viscosity η[31,32],

$$\eta_{\mathrm{red}} = \frac{\eta_{\mathrm{sp}}}{c} = \frac{\eta/\eta_0 - 1}{c} = [\eta] + k_h[\eta]^2 c \tag{1}$$

where η_{red} is the reduced viscosity, η_{sp} is the specific viscosity, η_0 is the solvent

viscosity, and $[\eta]$ is the intrinsic viscosity.

The Huggins coefficient provides a good starting point for understanding the link between PPI and viscosity since there are theories for relating k_h to simplified models for the colloidal interaction potential[31,33,34]. However, only a few measurements have been reported in literature. Some early studies to determine the protein intrinsic viscosity reported the slope of Equation 1, $k_h[\eta]^2$ [35,36,37], but did not discuss the physical meaning of the parameter. Monkos[38,13,39,40] provided useful data sets on the viscosity of unbuffered solutions of several albumins and immunoglobulins and also derived a model for calculating k_h as a function of temperature using a modified Arrhenius equation. However, no attempt was made to link k_h to protein properties or PPI. Of most relevance to this study, Yadav et al[14] presented k_h results for a set of four mAbs at pH 6.5 15mM NaCl. The interaction parameter, k_D, the zeta potential and the high concentration viscosity were also measured. While the zeta potential did not correlate to the k_h, a correlation was observed where larger k_h values were found for solutions with attractive PPI and greater viscosities at high protein concentrations. More recently, Pathak et al[41] found that colloidal models could not capture the relationship between protein-protein interactions and k_h for a series of 3 mAbs, which was attributed to the inability to account for solvation effects. In that work, intrinsic viscosity measurements indicated significant variation in protein conformation and structure with altering solution conditions, which could provide another reason why colloidal models were unable to describe the mAb behaviour.

The limited use of the k_h for understanding factors controlling concen-

trated solution viscosity could be related in part to challenges in experimentally measuring k_{h}. There can be inaccuracies in the calculation of k_{h} from applying the linear model to curved data and from compounding uncertainty from the instruments used to measure concentration and viscosity[42,13,43]. When applied to the viscosity data collected for proteins, the linearised form of the Huggins equation can yield negative values which are difficult to interpret[44] and published values can differ greatly from one another (See Supplementary Information for a table of BSA $[\eta]$ and k_{h} values at pH 5 and pH 7). Precise measurements of k_{h} would allow us to examine whether or not colloidal models are applicable for describing the viscosity of protein solutions.

Consequently, in this investigation a novel method for measuring the intrinsic viscosity and Huggins coefficient is developed and applied to BSA and two mAbs, PPI03 and PPI19. We show that measured values of k_{h} are in close agreement with predictions of colloidal sticky hard-sphere models for BSA and for PPI03, while models which account for anisotropic shape and interactions are more applicable for PPI19. We observe a very strong correlation of the k_{h} to high concentration viscosity and we rationalize why the correlation of viscosity with the protein-protein interaction parameters, k_{D} or B_{22}, is much weaker.

2. Materials & Methods

2.1. Protein Preparation

All buffer components used in this study are analytical grade. Sodium Acetate (NaAce), histidine (His), TRIS and sodium phosphate are used as

buffering agents. Sodium chloride (NaCl) and sodium thiocynate (NaSCN) are used to adjust ionic strength.. Phosphate buffer used in SEC-MALS-VISC experiments was made up as a solution of 38 mM Na_2HPO_4 12 mM NaH_2PO_4 150 mM NaCl. For all other buffers, the appropriate weight of buffer salt for the pH and ionic strength listed in the text was calculated based on the ionization state of the buffer. This amount was weighed out and added to deionised Milli-Q water of resistivity 18.2 Ω. The solution was then titrated to desired pH using an appropriate acid, acetic acid for NaAce buffers and hydrochloric acid (HCl) for other buffers. After preparationn, solutions were filtered under vacuum using a 0.22 µm Durapore PVDF membrane filter (Merck Millipore, Germany).

Monoclonal antibodies were kindly provided to the PIPPI consortium by AstraZeneca, Cambridge, UK. PPI03 and PPI19 are IgG_1 molecules with a molecular masses of 144.8 kDa and 147.6 kDa respectively. PPI03 appears in several studies as PPI03[45,46,47,48,49,50], mAb A[21], mAb 1[51,52] or PPI03[53,54,55]. PPI19 appears in other investigations as mAb B[21] and PPI19[55]. Monoclonal antibodies were dialysed into the desired buffer at 4 °C using 20 kDa MWCO Slide-A-Lyzer cassettes (Thermo Fisher Scientific, Dartford, UK) against a total buffer volume of 1000 times sample volume, in three solvent exchange volumes of 500 mL, 500 mL and 1 L over 24 hours. Post-dialysis samples were filtered using a Anotop syringe top filter (Merck Millipore, Germany) of 0.22 µm. Samples intended for use in SEC-MALS-VISC experiments were diluted to 1 mg mL^{-1} using the final dialysate.

BSA (heat shock fraction, pH 7, ≥98% purity) was purchased in crystalline from Sigma Aldrich. BSA was dissolved in the target buffer, then dialysed as

described above to remove any residual impurities. BSA was successively filtered with a 0.22 µm then 0.02 µm Anotop syringe top filter (Merck Millipore, Germany) and degassed under vacuum for 30 minutes before analysis.

2.2. Size exclusion chromatography with multi-angle light scattering and differential viscometry (SEC-MALS-VISC) for the measurement of intrinsic viscosity

Size exclusion chromatography coupled with multi-angle light scattering and differential viscometry (SEC-MALS-VISC) was performed to measure the intrinsic viscosity of the proteins. The instrument train was set up to include an Agilent G7110B HPLC pump, degasser and autoinjector (Agilient, Santa Clara, USA), Superdex 200 10/30 GL column (Cytiva, Marlborough,USA), miniDAWN TREOS MALS detector, ViscoStar III differential viscometer, and Optilab rEX refractive index meter (Wyatt, Santa Barbara, USA). A filter of 0.22 µm was inserted between the pump and autoinjector to filter solvent inline. Flow was set at 0.5 mL min^{-1} with mobile phase of pH 6.5 10 mM HisHCl 70 mM NaCl and sample volumes of 50 µL were injected. Additional SEC-MALS-VISC experiments were performed on PPI03 and PPI19 using the same detector array and method, but with an Acquity UPLC® pump, injector and UV detector (Waters, Elstree, UK) and a mobile phase of pH 7.4 38 mM Na_2HPO_4 12 mM NaH_2PO_4 150 mM NaCl.

2.3. Multi-injection Differential Viscometry (MIDV) for the measurement of intrinsic viscosity and Huggins coefficient

Huggins coefficient measurements were performed using an Agilent G7110B HPLC pump, degasser, inline solvent filter (0.22 µm) and autoinjector con-

nected with small bore PEEK tubing (0.127 mm) to a ViscoStar III and Optilab rEX for concentration measurement. Prior to analysis, the system and instrument train is flushed with the buffer of the sample being analysed using the pre-installed Wyatt buffer exchange method in ASTRA v.7[56]. The flow was set to $1\,\mathrm{mL\,min^{-1}}$ and temperature was maintained at 25 °C. Successive volumes of 100, 90, 80, 70, 60, 50 and 25 µL of the protein sample from the same vial were injected. The stock protein sample concentration was approximately $25\,\mathrm{mg\,mL^{-1}}$. Measurements were performed in triplicate for each solution condition for each mAb.

All data were collected and analysed using the ASTRA v.7 software. Additional analysis for the MIDV method was performed using a custom Python 3.6 script. The analysis script automatically split the raw data files in which the data from 7 successive injections of decreasing mass are recorded into the respective peaks using the auto-inject signal data as boundary markers for the peaks. The area of the refractive index and specific viscosity peaks was computed by numerically integrating across the peak using the trapezoidal function. The total mass of the concentration peak was calculated by dividing the area of the integrated refractive index peaks by the $\frac{dn}{dc}$ of protein solutions, which is approximately equal to $0.185\,\mathrm{mL\,g^{-1}}$ in these conditions, and the dilution factor of the ViscoStar instrument which was 0.54. The intrinsic viscosity and k_h were evaluated by using the minimize function from the lmfit Python library to fit the model in Equation 8 to the data collected from the viscometer and the total mass values from the concentration peaks.

2.4. Microfluidic Rheometry for the Measurement of Solution Viscosity

Microfluidic rheometry experiments were carried out using an mVROC® Initium automated sampling microfluidic rheometer-on-a-chip platform (Rheosense, San Ramon, CA, USA). A stock protein sample at $180\,\mathrm{g\,L^{-1}}$ was prepared by dialysis following the method described above, then serially diluted using dialysate from the final buffer exchange. The concentration range in this study was between 1.6 and $30\,\mathrm{mg\,mL^{-1}}$ for samples of PPI03 and between 5 and $25\,\mathrm{mg\,mL^{-1}}$ for samples of BSA. Concentration measurements were taken using a NanodropOne (Thermo Fisher Scientific, Dartford, UK). The samples were loaded into the mVROC® vial inserts and placed in the autosampler tray. A B05 chip was used with a syringe size of 100 µL. Temperature was set to 23°C. For BSA, the loaded sample volume for each run was 20 µL. Each sample was measured in triplicate giving a total sample consumption of 60 µL. The shear rate was $18\,500\,\mathrm{s^{-1}}$. Sample volume was 50 µL for PPI03 samples, at a shear rate of $2000\,\mathrm{s^{-1}}$. In all cases studied, the measurements exceed 10% of the full scale capacity of the chip. The viscosity was measured at a series of shear rates to confirm the solution viscosity measured was independent of shear rate (data not shown). The Péclet (Pe) numbers of the solutions of BSA and PPIO3 used in the validation experiments were 0.0136 and 0.0057 respectively, below the threshold of $\mathrm{Pe} = 1$ indicative of shear thinning. An exploration of the shear-dependency of viscosity in solutions of concentrated PPI03 and PPI19 is published in Lanzaro et al[54]. Data were collected using the Rheosense software and exported to Origin 2020 where the data were plotted and parameters derived from the fit of Equation 1 to the data.

3. Development of the Multi-Injection Differential Viscometry Method for the measurement of Intrinsic Viscosity and the Huggins coefficient

The use of differential viscometers to determine the intrinsic viscosity of polymers and proteins is an established technique[57,43]. The sample is separated by size exclusion chromatography, the specific viscosity across the sample peak is measured by a differential viscometer and the concentration across the peak is measured either by UV or refractive index detection. At the dilute protein concentrations of 0.1-0.5 $\mathrm{mg\,mL^{-1}}$ eluting from a SEC column, only the intrinsic viscosity is measured. The contribution to the reduced viscosity by second order interactions, described in the $k_h[\eta]^2c$ term of the Huggins Equation, is negligible at these low concentrations and therefore k_h cannot be determined.

To measure both $[\eta]$ and k_h, higher concentration sample injections are required. The SEC column must be removed when injecting high protein concentration samples as this causes overloading of the column, incomplete separation and a distorted and asymmetric signal peak. When injecting without a column at higher protein concentrations band-broadening corrections, which account for the broadening of the peak as it moves between detectors, cannot be applied as the shape of the specific viscosity peak is altered by the higher order, two-body interactions as quantified by the $k_\mathrm{h}[\eta]^2c$ term in Equation 1. An alternative approach is to calculate the k_h from the total peak areas of the signal traces of both the viscometer and the concentration detectors expressed in terms of the total mass of injection, as the total peak area is not affected by band broadening.

The total mass of the injection from the concentration signal is calculated by integrating the peak and dividing by the $\frac{dn}{dc}$. Assuming that the concentration is small enough that terms of order c^3 are negligible, the concentration-dependence of solution viscosity is written as the Huggins equation:

$$\frac{\eta}{\eta_0} = 1 + [\eta]c + k_h[\eta]^2c^2 \tag{2}$$

Factorising for $[\eta]c$ gives

$$\eta_{sp} = [\eta]c(1 + k_h[\eta]c) \tag{3}$$

and upon rearrangement,

$$\frac{\eta_{sp}}{[\eta]}\frac{1}{(1 + k_h[\eta]c)} = c \tag{4}$$

The denominator in Equation 4 can be expanded in a Taylor series as long as $k_\mathrm{h}[\eta]\mathrm{c}\ll 1$ to give

$$\frac{\eta_{sp}}{[\eta]}(1 - k_h[\eta]c) = c \tag{5}$$

$[\eta]c$ can be approximated as

$$[\eta]c = \eta_{sp} + O((k_h[\eta]c)^2) \tag{6}$$

This approximation can then be used in Equation 5. Omitting the negligible $O((k_h[\eta]c)^2)$ terms

$$c \approx \frac{\eta_{sp}}{[\eta]}(1 - k_h\eta_{sp}) \tag{7}$$

In this form, the concentration is expressed in the terms of the specific viscosity measurement from the differential viscometer. To express Equation 7 in terms of the total mass injected, the signal is integrated across the peaks,

$$m_{inj} = \int c(t)dt = \frac{1}{[\eta]} \int \eta_{sp}(t)dt - \frac{k_h}{[\eta]} \int \eta_{sp}(t)^2 dt \quad (8)$$

From one vial of protein solution, a HPLC autosampler injects series of different protein masses and the results are recorded. This reduces manual input and makes the measurements more reliable and reproducible. The model described in Equation 8 is fit with the integrated concentration, specific viscosity and specific viscosity squared peak data from all injections to determine the values for k_h and $[\eta]$.

4. Results

4.1. Validation of Protocol for the Measurement of the [η] & k_h by MIDV

Multi-Injection Differential Viscometry (MIDV) was developed and qualified using samples of BSA and the antibody PPI03. The intrinsic viscosity and Huggins coefficient of the samples were validated against measurements made by microfluidic rheometry. Results and uncertainty of the parameters from the fit are listed in Table 1. The plots of the fit of Equation 1 to the viscosity data measured by microfluidic rheometry with 95% confidence intervals are shown in Figure 1a and Figure 1b. These figures also include the viscosity curves simulated using parameters derived from fitting data collected using MIDV to Equation 8, with error bars from the propagation of the uncertainty of the fitted parameters, $[\eta]$ and k_h.

The average intrinsic viscosity of BSA obtained by MIDV is in good agreement with the value obtained from microfluidic rheometry, the value of $4.15\,\mathrm{mL\,g^{-1}}$ measured for this sample by SEC-MALS-VISC and the published value of $4.2\,\mathrm{mL\,g^{-1}}$ corresponding to BSA in similar formulation conditions[58].

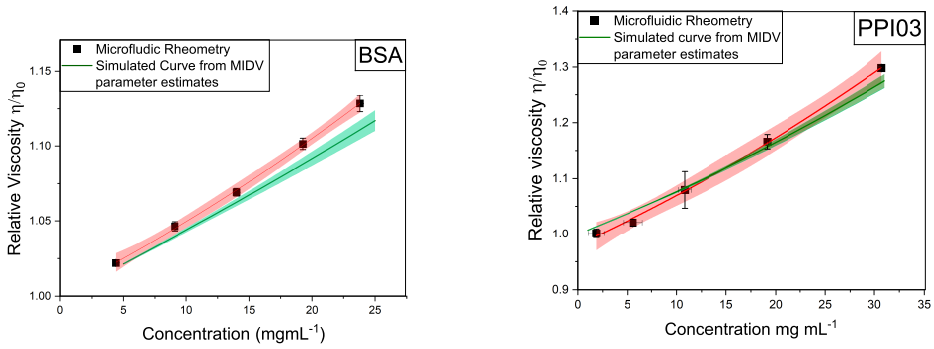

(a) (b)

Figure 1: Comparison of data collected by microfluidic rheometry and MIDV for a) BSA in pH 7.4 phosphate buffered saline 200 mM total ionic strength and b) PPI03 in pH 5 25 mM sodium acetate buffer. Red shading shows 95% confidence intervals of the fit of Equation 1 to the microfluidic rheometry data. Green shading represents the uncertainty in the simulated curves from the propagated uncertainty of the fitted parameters from the MIDV data.

Method	$[\eta]$ **(mL g^{-1})**	**+ / -**	$\boldsymbol{k_h}$	**+ / -**
BSA MIDV Run 1	4.20	0.013	1.085	0.095
BSA MIDV Run 2	4.20	0.015	1.021	0.109
BSA MIDV Run 3	4.19	0.021	1.101	0.157
BSA Microfluidic Rheometry	4.18	0.511	2.609	1.646
PPI03 MIDV Run 1	7.21	0.017	0.894	0.056
PPI03 MIDV Run 2	7.18	0.013	0.865	0.044
PPI03 MIDV Run 3	7.09	0.025	1.139	0.074
PPI03 Microfluidic Rheometry	8.16	1.25	1.08	0.55

Table 1: Parameter values from MIDV and microfluidic rheometry measurements made on samples of BSA in PBS at pH 7.4 200 mM and PPI03 in pH 5 25 mM sodium acetate buffer. k_h is dimensionless in units of $[\eta]c$.

The intrinsic viscosity value measured for the PPI03 pH 5 sample by MIDV is within the uncertainty of the microfluidic rheometry value also and is close to the values of 6 to 7 mL g^{-1} reported in the literature for mAbs[12,13,14,15].

The average k_h value measured for BSA by MIDV is 1.07. The measured value for the MIDV method is within the uncertainty of the microfluidic rheometry value. At the high ionic strength and neutral pH conditions of this experiment, BSA molecules are likely to have minimal interactions and to behave as hard ellipsoids[59]. The MIDV k_h value for BSA is close to the theoretical hard sphere limiting value of approximately one[31,34]. The measured value is lower than the k_h of 2.1 reported by Tanford[35] at pH 7 100mM and the k_h of 1.58 reported by Curvale[44] for a sample at pH 7 with low ionic strength. The Huggins coefficient values listed in Table 1 for samples

of PPI03 pH 5 derived from the MIDV data are also within the uncertainty of k_{h} determined by the microfluidic rheometry.

MIDV values show good reproducibility for both $[\eta]$ and k_{h} between replicate runs and results were in agreement with orthogonal techniques. The uncertainty of k_{h} is an order of magnitude less by MIDV compared with the values measured by microfluidic rheometry. These results confirm the applicability of MIDV to measure the $[\eta]$ and k_{h} in protein samples.

A key assumption of the MIDV method is that there exists a linear relationship between η_{red} and c over the experimental protein concentration range (see Equation 1). For conditions with strong electrostatic repulsion, the $\eta_{red}(c)$ profile becomes non-monotonic exhibiting a maximum at low protein concentration, which is known as the secondary electroviscous effect[60]. As such, the increase in $[\eta]$ for PPI03 at pH 5 is possibly an artefact of neglecting this effect, although it is not possible to detect any non-linear relationship in η_{red} as a function of c using the data measured by microfluidic rheometry (see Figure 1b). According to Heinen *et al.*[60], for BSA solutions without any added salt, η_{red} exhibits a maximum between 1 and 3 g/L. The PPI03 condition at pH 5 is at a much higher ionic strength of 25 mM, which corresponds to much weaker electrostatic repulsion. A more equal comparion would be with intrinsic viscosity data reported by Pindrus *et al.*[57], who reported a similar change in $[\eta]$ for a mAb at pH 4 when increasing ionic strength from 15 mM (6.4 mL g^{-1}) to 150 mM (5.9 mL/g). The other possibility is that $[\eta]$ decreases with increasing ionic strength due to screening intramolecular electrostatic repulsion leading to a reduced hydrodynamic volume of the protein. This change in size would also be reflected by a decrease in the infinite dilution

hydrodynamic radius $R_{H,0}$ determined by dynamic light scattering, which is not observed for PPI03[52]. As such, the value of k_H for PPI03 at pH 5 with should be considered an apparent value. For PPI19, there is a significant increase in the measured $R_{H,0}$[21], which could explain the increase in $[\eta]$ measured at pH 5.

4.2. Correlating dilute solution measurements to high concentration viscosity

The main motivation of this work is to examine whether concentrated solution viscosity correlates to k_h. As shown in the previous section, $[\eta]$ is measured concurrently with k_h and an exploration of the effects of the solution conditions studied on the $[\eta]$ is included in Supplementary Information.

Previous studies have correlated B_{22} or k_D with a representative high concentration viscosity, usually between 100 and 250 mg mL^{-1} [10,61,27,29]. Here, we follow the approach used by Connolly[17] and Shah[55], where the dilute solution parameters are correlated with the exponential viscosity coefficient, k_{exp}, obtained by fitting our concentrated-solution viscosity data reported in Lanzaro *et al.*[54] with the following model,

$$\eta_R = \frac{\eta}{\eta_0} = e^{k_{exp}c} \tag{9}$$

where c is mAb concentration. Connolly et al[17] demonstrated that describing viscosity data in this way helped to reduce the effect of noise associated with the difficulties in measuring concentration and viscosity in concentrated protein solutions. The viscosity values used in the fitting are averages over the zero-shear viscosity plateau, where shear thinning behaviour was observed at higher shear rates for solution conditions corresponding to strong protein-protein association[54].

The values of k_{exp} for two mAbs PPI03 and PPI19 in a variety of solution conditions are given in Table 2 and have been previously reported by Shah[55]. The MIDV measured values for $[\eta]$ and k_h are also listed. The protein-protein interaction parameter, k_D and the dimensionless osmotic second virial coefficient, b_{22}, included in Table 2 were reported in previous studies for PPI03[52,51,55] and for PPI19[54,55]. Here, $b_{22} = B_{22}/B_{22}^{ex}$, where B_{22} is the osmotic second virial coefficient and B_{22}^{ex} is the excluded volume contribution, which is approximately equal to 7 x 10^{-5} mol mL g^{-2} for both mAbs[21].

Condition	$[\eta]$ **(mL g^{-1})**	k_h	k_D **(mL g^{-1})**	b_{22}	k_{exp} **(mL g^{-1})**
PPI03 pH5	7.16 +/- 0.08	0.97 +/- 0.08	16.7 +/- 0.8	2.40 +/- 0.09	10.6 +/- 0.1
PPI03 pH5 250 mM NaCl	6.60 +/- 0.08	0.75 +/- 0.10	-5.1 +/- 0.5	0.17 +/- 0.02	10.4 +/- 0.4
PPI03 pH 5 250 mM NaSCN	6.49 +/- 0.09	1.25 +/-0.07	-8.4 +/- 0.4	-0.12 +/- 0.02	13.0 +/- 0.2
PPI03 pH 6.5	6.73 +/- 0.05	0.87 +/- 0.07	4.0 +/- 0.3	1.21 +/- 0.03	13.5 +/- 0.5
PPI03 pH 9 Tris	6.37 +/- 0.07	2.46 +/- 0.20	-11.3 +/- 0.6	-0.43 +/- 0.02	18.3 +/- 0.5
PPI19 pH5 25 mM NaCl	7.82 +/- 0.08	3.01 +/- 0.32	-18.6 +/- 0.8	-2.70 +/- 0.21	25.1 +/- 0.3
PPI19 pH5 250 mM NaCl	7.02 +/- 0.03	2.11 +/- 0.05	-18.4 +/- 0.8	-3.03 +/- 0.16	18.5 +/- 0.1
PPI19 pH8 250 mM NaCl	7.31 +/- 0.13	1.59 +/- 0.17	-17.3 +/- 1	-2.20 +/- 0.13	16.5 +/- 0.3

Table 2: Values of the intrinsic viscosity, the Huggins coefficient, k_h, which is dimensionless, the interaction parameter, k_D, the dimensionless reduced second osmotic virial coefficient, b_{22} and the viscosity exponential coefficient k_{exp} for solutions of PPI03 and PPI19.

The correlations of k_{exp} to k_D and b_{22} are plotted in Figure 2 a) and b) respectively, while Figure 3 illustrates the relationship between k_h and k_{exp}. Also included in the correlation plots in Figures 2 and 3 are data of four mAbs at pH 6 15 mM ionic strength from Yadav et al.[14].

There is a strong correlation between dilute and concentrated solution viscosity for solution conditions where the net protein-protein interaction

potential ranges from repulsive to strongly attractive. The k_h correlates much more strongly with the k_{exp} according to the Pearson's correlation coefficient equal to 0.99 (0.84 including data from Yadav et al (2010)[14], 0.99 when the outlier mAb A is excluded from the fit), compared to values of -0.77 and -0.62 (-0.60 including data from Yadav et al (2010)[14]) obtained from the relationship with b_{22} or k_D, respectively. While the Pearson's correlation coefficients for all of these data sets indicate good correlations, the high value for the k_{exp}-k_h correlation demonstrates k_h is the most reliable parameter studied to link dilute solution behaviour and concentrated solution viscosity. There is good agreement with our k_{exp}-k_h correlation for the samples mab G and mAb E from the Yadav (2010)[14] data set. Even mAb H, which exhibits a much higher viscosity and corresponding value of k_h than the most viscous PPI19 sample, adheres well to the correlation.

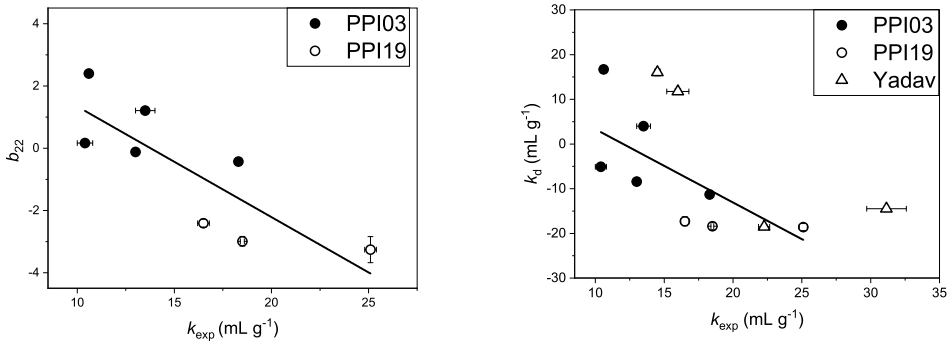

(a) (b)

Figure 2: Correlation of k_{exp} to **a)** b_{22} and **b)** k_D for PPI03, PPI19 and four mAbs at pH 6.5 15 mM NaCl taken from Yadav et al. 2010[14]. The solid line represents the correlation of k_{exp} with b_{22} and k_h respectively, including only the data collected by MIDV as part of this study.

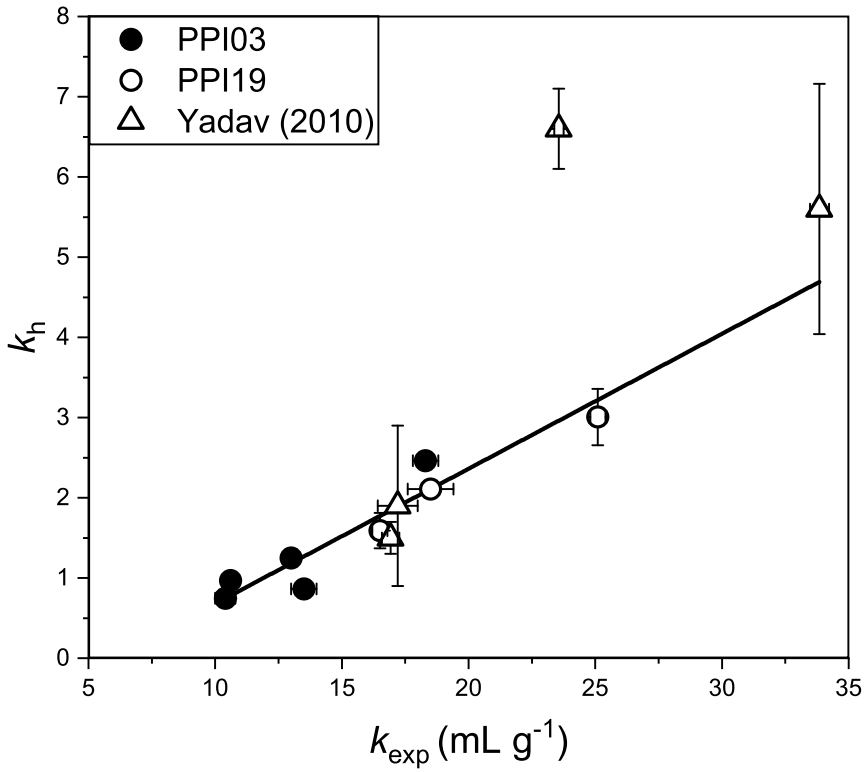

Figure 3: Correlation between the Huggins' coefficient, k_h, and the exponential fit parameter, k_{exp} for PPI03 and for PPI19 and for mAb A, mAb H, mAb G and mAb E from Yadav (2010)[14] .

Generally, poor rheological behaviour and viscous solutions occur at high protein concentrations in the presence of attractive protein-protein interactions[62,63,64]. However, we find a lack of a correlation between PPI measurements, represented by k_D and b_{22}, and the concentrated solution viscosity when considering the viscous samples where $k_{exp} > 15$ mL g^{-1}. For these solution conditions, the range of k_D values is between -14.5 and -18.6 mL g^{-1}, while values of k_{exp} increase from 16.5 to 34 mL g^{-1}. The k_D values for all PPI19 samples are similar, but the PPI19 pH 5 0 mM NaCl sample is much more viscous than the other solutions. On the other hand, protein-protein interactions are much less attractive for PPI03 pH 9 sample when compared to any of the PPI19 solutions, but the viscosity for PPI03 at pH 9 is similar to the high ionic strength samples of PPI19. Lastly, while the samples of mAb-H appear much more viscous than any condition for PPI19, the reported k_D value equal to -14.5 mL g^{-1} indicates the averaged protein-protein interactions are less attractive. While these large discrepancies exist when correlating the k_D measurements, there is a very strong correlation across these conditions when using k_h. The only exception is mAb-A, which exhibits a very high value of k_h, but not a proportionally large k_{exp}.

4.3. The k_h of protein solutions is related to protein-protein interactions

A key aim of this work is to elucidate the relationship between the k_h and protein-protein interactions, which can be tuned by changing the solution pH and ionic strength to alter the relative contribution from short-ranged attractions and a long-ranged electrostatic repulsion. The plot of the relationship between b_{22} and k_h for BSA, PPI03 and PPI19 is provided in Figure 4. Also given are the predictions from colloidal models of the relationship between

b_{22} and k_h which we can use as a starting point to understand the effects of PPI on k_h [31,33,34,65,66]

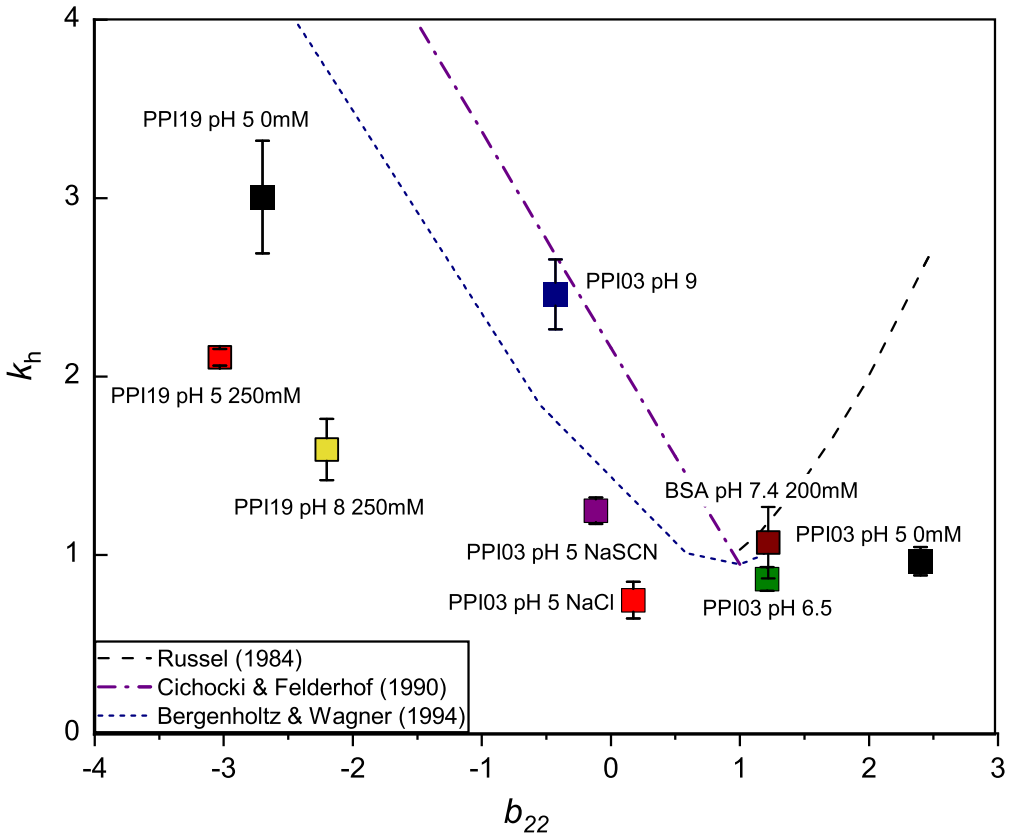

Figure 4: Correlation of protein-protein interactions in PPI03 and PPI19, represented by b_{22}, to the Huggins coefficient, k_h

The Huggins coefficient is expected to have a value of one for a hard sphere which corresponds to a b_{22} of one in the approach taken by Russel, Cichoki and Felderhof, Bicerano et al. and Krishnamurhty et al. [31,33,65,66]. Fitting to structure factors obtained from small angle X-ray scattering measurements

indicates BSA and HSA do not exhibit any short-ranged attractive interactions at conditions similar to the BSA sample in Figure 4 making it a good representative of a colloid interacting with a hard sphere potential[59,67]. The measured value of $k_{\mathrm{h}} \approx 1$ for the BSA sample is therefore in good agreement with theory for hard spheres.

Russel[31] accounted for longer-ranged repulsive interactions by calculating k_{h} for an excluded-shell model where the hard sphere potential extends past the hydrodynamic radius of the protein to match the b_{22} value. This results in a prediction for k_{h} which rises rapidly with increasingly repulsive b_{22}. PPI03 at pH 5 and low ionic strength is the only condition we investigated where $b_{22} > 1$. For this condition, we find the measured value of k_{h} is overestimated by the excluded-shell model. This result is not surprising since the Huggins analysis might not be applicable to this condition due to the lonranged nature of the electrostatic repulsion. An improved prediction of the low-concentration viscosity requires modelling the repulsion with a screened yukawa potential following the approach described by Heinen *et al*[60], which is beyond the scope of our study.

The predictions for colloids exhibiting net attractive interactions, where k_{h} increases with decreasing b_{22}, are also shown in Figure 4. The longer-dashed lines correspond to the approach of Cichocki and Felderhof[33] where k_{h} has been determined for the Baxter model, which corresponds to limiting case of sticky hard spheres. In this limit, the relationship of k_{h} to b_{22} is given by[33],

$$k_{\mathrm{h}} = 2.161 - 1.215\ b_{22} \tag{10}$$

The shorter-dashed lines in Figure 4 are the Bergenholtz-Wagner[34] prediction,

which corresponds to colloids interacting through an attractive square-well potential, where the range of the potential normalised by the colloid radius is equal to 0.15.

We have previously shown that simplified spherical models, based on an adhesive Baxter potential provide an accurate representation for the thermodynamic properties for PPI03 over a large protein concentration range under conditions where $b_{22} < 1$ [54,53]. For the strongly attractive PPI03 pH 9 condition, the predictions of the colloidal models based on isotropic short-range attractive Baxter potentials provide an accurate estimate for k_{h}. The measurements of k_{h} for PPI03 pH 5 250 mM NaSCN agree more closely with the calculations of the square well model versus the sticky sphere limit, which predicts a more rapid increase in k_{h} versus b_{22}. For systems which are weakly attractive and have relatively large normalised well-widths of 0.1 or greater, Bergenholtz highlighted a likelihood of overestimation of the k_{h} parameter of more than 100% when using the sticky-sphere model[34]. It was demonstrated that for all well widths, the attractive square-well structures were perturbed less by shear than the hard sphere solutions and the resulting net change in both hydrodynamic and thermodynamic stress yielded a lower k_{h} than the sticky sphere prediction[34].

The only condition for PPI03 where an increase in protein-protein attraction does not lead to an increase in k_{h} is for solutions at pH 5 with 250 mM NaCl. For this condition, the addition of salt screens repulsive electrostatic interactions leading to a relatively weak short-ranged attraction. A reduction in k_{h} below the hard sphere value has been predicted by Bergenholtz and Wagner[34]. In the presence of a small net attractive force there is a positive

hydrodynamic contribution but a larger negative thermodynamic contribution in the square well model resulting in lower k_h value for weakly attractive solutions compared to the hard-sphere k_h of 0.946. A recent study on the microrheology of a model colloidal particle in a Newtonian solvent varied b_{22} value for the particle and calculated the microviscosity for each condition. In agreement with the Bergenholtz findings, Huang *et al.*[68] determined that the minimum in microviscosity occurs in the region where there is a small attractive force, specifically at b_{22}= 0.25[68]. The k_h minimum for PPI03 occurred at a similar b_{22} value of 0.17 for the weakly attractive PPI03 pH 5 250mM NaCl solution.

The b_{22} values for PPI19 indicate much stronger attractive interactions than observed for PPI03 under all solution conditions, although the measured k_h values are not proportionally greater. Correspondingly, the k_h values are significantly over-predicted by the isotropic colloidal models shown in Figure 4. In Lanzaro et al.[54], the behaviour of PPI19 could only be satisfactorily captured using chemical association models including the formation of reversible small oligomers (dimers or trimers) at lower protein concentrations. This type of behaviour has also been observed for many other mAbs that exhibit strong reversible self association[69,22,10,61,18]. For reversibly associating mAbs, it is not surprising that b_{22} and k_h do not correlate. k_h values will reflect the oligomer structure, where more open versus compact oligomers contribute more to viscosity due to having greater effective volumes and correspondingly higher intrinsic viscosities[10]. On the other hand, for strongly associating systems, because b_{22} values are obtained from the osmotic compressibility profiles, the parameters reflect the decrease in protein number concentration

due to oligomerization or the average association state of the protein, but do not contain any information about the oligomer hydrodynamic properties such as their compactness.

5. Discussion

A key question to consider is why should k_{h} correlate better with concentrated solution viscosity than k_{D} and b_{22} which are direct measures of protein-protein interactions. We expect there are a number of reasons, which in part, depend on whether the comparison is being made across different mAbs or for the same mAb, but across different solution conditions.

For PPI03, the lack of a correlation between concentrated solution viscosity and b_{22} is most apparent when considering the conditions in which the $b_{22} > 0.5$, where the main effect of changing solution conditions is to alter repulsive electrostatic interactions. For example, increasing the salt concentration of a PPI03 solution at pH 5 significantly impacts PPI due to screening electrostatic interactions leading to a large drop in b_{22}. However, there appears to be little impact on k_{exp} when ionic strength is increased from 25 mM to 250 mM. We find that the value of k_{h} is a much better predictor for concentrated solution viscosity than measures of PPI as there is only a small difference between k_{h} values for PPI03 at pH 5 0 mM NaCl and PPI03 pH 5 250 mM NaCl. A number of other studies have shown that concentrated solution viscosity is relatively insensitive to alterations in the electrostatic repulsion between proteins above a threshold of approximately 15 mM[60,70,71,72,73]. At high protein concentrations, the increased counter-ion concentrations are expected to screen any electrostatic repulsion leading to

the weak dependence of viscosity on ionic strength[60].

Another example where the repulsive electrostatic interactions impact b_{22} differently than k_{h} is for PPI19 at pH 5 under low ionic strength conditions, which corresponds to conditions where we expect the protein-protein interaction is composed of a combination of short-ranged attraction and long-ranged electrostatic repulsion. PPI19 phase separates at higher pH values and low ionic strength conditions due to strong attractive PPI[21]. Reducing the pH to 5 increases the net positive charge on the protein and prevents phase separation, reflecting the electrostatic repulsion between PPI19 molecules. The value of the net interaction parameters b_{22} = -2.70 or $k_{\mathrm{D}} = -18.6\,\mathrm{mL\,g^{-1}}$ are sufficiently less than 0 to indicate a strong protein-protein attraction is in balance with the large electrostatic repulsion. Previous studies have shown that proteins exhibiting short-range attractive long-range repulsive potentials form reversible clusters, which cause high viscosities at high protein concentrations[74,22,75,76]. The correlation between k_{h} and the high concentration viscosity of this sample shows that the dilute solution viscosity reflects the effects of this cluster formation. However, the electrostatic repulsion is not evident from the values of k_{d} or b_{22}, which are similar for conditions at low and high salt concentration.

For conditions with net attractive protein-protein interactions, b_{22} does not correlate with viscosity at low protein concentrations (as characterized by the k_{h} value), so the lack of a correlation with high concentration viscosity is not surprising. On the other hand, we have found that k_{h} correlates with concentrated solution viscosity for PPI03 and for PPI19 as well as for three out of the four mAbs investigated by Yadav et al.[14]. This result

is unexpected because concentrated solution viscosity has been attributed to the structures or effective volumes of transient protein clusters, which are predominantly formed only at high protein concentrations[10]. Indeed differences in the effective volume of protein clusters formed at high protein concentration and the oligomers formed at low protein concentration could explain why mAb A does not follow the k_{h} correlation. Yearley et al. (2014)[69] showed that at low protein concentrations mAb A forms a dimer with a high effective volume (an elongated structure), which would lead to a large k_{h} value. On the other hand, at higher protein concentrations the rotational freedom of mAb A is restricted and prevents the anisotropic electrostatic self-association[25]. This could arise if the dimers are forced to adopt more compact conformations as the solution becomes more crowded leading to a lesser excluded volume contribution to viscosity. Conversely, we hypothesize that the correlation between k_{h} and concentrated solution viscosity exists when the structures of the transient clusters formed at high protein concentration are self similar to the oligomer structures formed at low protein concentrations.

6. Conclusions

Understanding the relationship between PPI and the viscosity of high concentration protein solutions is key in designing good quality protein formulations. This field has been limited so far by prohibitive protein requirements for viscosity measurements and by conflicting results when correlating dilute solution thermodynamic parameters, k_{D} and b_{22}, to high concentration solution behaviour.

We have introduced a technique for the determination of the Huggins

coefficient and intrinsic viscosity of protein solutions. The measurement of intrinsic viscosity and k_h agreed with literature and measurements by orthogonal methods. The improved precision of MIDV is demonstrated by the order of magnitude difference in uncertainty between MIDV values and comparable measurements using microfluidic rheomtery. The method is significantly less labour-intensive than measuring k_h using current methods as there is no requirement for sample upconcentrating, manual dilution series or independent concentration measurements and the entire process can be automated using a HPLC system.

The protein material requirements for MIDV are also favourable. In this proof-of-concept study, a single 500 µL sample of intermediate concentration of 25-30 $\mathrm{mg\,mL^{-1}}$ was all that was required to generate a value for $[\eta]$ and k_h. It is highly likely that further optimisation would substantially reduce the total protein mass needed, not least as the method could be transferred to the microViscostar, a differential viscometer designed to measure at the minimal sample volumes associated with UHPLC analysis.

The exponential viscosity coefficient, k_{exp} was used to compare correlations of concentrated solution viscosity to dilute solution parameters between proteins and formulations. Our key finding is that the correlation between k_{exp} and k_h is much stronger than with either k_D or b_{22}. The strong correlation suggests k_h provides a better indicator for the transient solution structure that is determined by the the hydrodynamic properties of the structural building blocks, which could be monomers or oligomers, the valency of the mAb-mAb interactions, or for conditions at low ionic strength, the relative contribution of long-ranged repulsion to the short-ranged protein-protein at-

tractions. These properties are not uniquely specified by b_{22} or k_d because the parameters only reflect the averaged protein-protein interactions and are not sensitive to the geometric properties of any oligomers formed at low protein concentrations. Furthermore, we have shown that correlations between b_{22} and dilute solution viscosity breakdown when manipulating repulsive electrostatic interactions, although there still exists a strong correlation between dilute and concentrated solution viscosity.

7. Acknowledgements

Aisling Roche and Lorenzo Gentiluomo were supported by EU Horizon 2020 Research and Innovation program under the Marie Skłodowska-Curie grant agreement No 675074. Nicole Sibanda was supported by an EPSRC DTP studentship (Ref. no. 2389795) with a financial contribution from AstraZeneca (MedImmune). The authors thank Alfredo Lanzaro, Daniel Corbett, Maryam Shah, Vanessa Schneider, Arthur Porfetye, Roger Scherrer and all the staff at Wyatt Europe, Pernille Harris and the ESRs and supervisors of the PIPPI consortium.

8. CRediT Author Statement

Aisling Roche: Conceptualization, Methodology, Software Writing, Investigation, Formal Analysis, Writing- Original Draft; **Lorenzo Gentiluomo:** Methodology; Writing - Review & Editing; **Nicole Sibanda** Investigation, Formal Analysis; **Dierk Roessner:**Resources; **Wolfgang Friesß:** Resources, Writing - Review & Editing, Supervision; **Steven P. Trainoff:**Conceptualization of MIDV Technique, Methodology, Writing - Review

& Editing; **Robin Curtis:** Conceptualization, Supervision, Writing- Review & Editing.

Figure 5: Graphical Abstract

References

[1] Steven J. Shire, Zahra Shahrokh, and Jun Liu. Challenges in the development of high protein concentration formulations. *Journal of Pharmaceutical Sciences*, 93(6):1390–1402, jun 2004. ISSN 00223549. doi: 10.1002/jps.20079.

[2] Patrick Garidel, Alexander B. Kuhn, Lars V. Schäfer, Anne R. Karow-Zwick, and Michaela Blech. High-concentration protein formulations: How high is high? *European Journal of Pharmaceutics and Biopharmaceutics*, 119:353–360, oct 2017. ISSN 18733441. doi: 10.1016/j.ejpb.2017.06.029.

[3] Herb Lutz, Joshua Arias, and Yu Zou. High concentration biotherapeutic formulation and ultrafiltration: Part 1 pressure limits. *Biotechnology Progress*, 33(1):113–124, jan 2017. ISSN 1520-6033. doi: 10.1002/BTPR.2334.

[4] Andrea Allmendinger, Stefan Fischer, Joerg Huwyler, Hanns Christian Mahler, Edward Schwarb, Isidro E. Zarraga, and Robert Mueller. Rheological characterization and injection forces of concentrated protein

formulations: An alternative predictive model for non-Newtonian solutions. *European Journal of Pharmaceutics and Biopharmaceutics*, 87(2): 318–328, jul 2014. ISSN 18733441. doi: 10.1016/j.ejpb.2014.01.009.

[5] Mahlet A. Woldeyes, Lilian L. Josephson, Danielle L. Leiske, William J. Galush, Christopher J. Roberts, and Eric M. Furst. Viscosities and Protein Interactions of Bispecific Antibodies and Their Monospecific Mixtures. *Molecular Pharmaceutics*, 15(10):4745–4755, 2018. ISSN 15438392. doi: 10.1021/acs.molpharmaceut.8b00706.

[6] Youngbin Baek, Nripen Singh, Abhiram Arunkumar, Michael Borys, Zheng J. Li, and Andrew L. Zydney. Ultrafiltration behavior of monoclonal antibodies and Fc-fusion proteins: Effects of physical properties. *Biotechnology and Bioengineering*, 114(9):2057–2065, sep 2017. ISSN 10970290. doi: 10.1002/bit.26326.

[7] Prasad S. Sarangapani, Steven D. Hudson, Kalman B. Migler, and Jai A. Pathak. The limitations of an exclusively colloidal view of protein solution hydrodynamics and rheology. *Biophysical Journal*, 105(10):2418–2426, nov 2013. ISSN 00063495. doi: 10.1016/j.bpj.2013.10.012.

[8] Andrea D. Gonçalves, Cameron Alexander, Clive J. Roberts, Sebastian G. Spain, Shahid Uddin, and Stephanie Allen. The effect of protein concentration on the viscosity of a recombinant albumin solution formulation. *RSC Advances*, 6(18):15143–15154, feb 2016. ISSN 2046-2069. doi: 10.1039/C5RA21068B.

[9] Jessica J Hung, Barton J Dear, Carl A Karouta, Amjad A Chowdhury,

P. Douglas Godfrin, Jonathan A Bollinger, Maria P Nieto, Logan R Wilks, Tony Y Shay, Kishan Ramachandran, Ayush Sharma, Jason K Cheung, Thomas M Truskett, and Keith P Johnston. Protein–Protein Interactions of Highly Concentrated Monoclonal Antibody Solutions via Static Light Scattering and Influence on the Viscosity. *The Journal of Physical Chemistry B*, 123(4):739–755, jan 2019. ISSN 1520-6106. doi: 10.1021/acs.jpcb.8b09527.

[10] Wenhua Wang, Wayne G Lilyestrom, Zhi Yu Hu, and Thomas M Scherer. Cluster Size and Quinary Structure Determine the Rheological Effects of Antibody Self-Association at High Concentrations. *The Journal of Physical Chemistry B*, 122(7):2138–2154, feb 2018. ISSN 1520-6106. doi: 10.1021/acs.jpcb.7b10728.

[11] Mitja Zidar, Petruša Rozman, Kaja Belko-Parkel, and Miha Ravnik. Control of viscosity in biopharmaceutical protein formulations. *Journal of Colloid and Interface Science*, 580:308–317, jul 2020. ISSN 10957103. doi: 10.1016/j.jcis.2020.06.105.

[12] Craig G Hall and George N Abraham. Reversible self-association of a human myeloma protein. Thermodynamics and relevance to viscosity effects and solubility. *Biochemistry*, 23(22):5123–5129, 1984. ISSN 0006-2960.

[13] K Monkos and B Turczynski. A comparative study on viscosity of human, bovine and pig IgG immunoglobulins in aqueous solutions. *International Journal of Biological Macromolecules*, 26(2-3):155–159, nov 1999. ISSN 01418130. doi: 10.1016/S0141-8130(99)00080-X.

[14] Sandeep Yadav, Steven J. Shire, and Devendra S. Kalonia. Factors affecting the viscosity in high concentration solutions of different monoclonal antibodies. *Journal of Pharmaceutical Sciences*, 99(12):4812–4829, dec 2010. ISSN 15206017. doi: 10.1002/jps.22190.

[15] J. Paul Brandt, Thomas W. Patapoff, and Sergio R. Aragon. Construction, MD simulation, and hydrodynamic validation of an all-atom model of a monoclonal IgG antibody. *Biophysical Journal*, 99(3):905–913, aug 2010. ISSN 15420086. doi: 10.1016/j.bpj.2010.05.003.

[16] Dheeraj S. Tomar, Sandeep Kumar, Satish K. Singh, Sumit Goswami, and Li Li. Molecular basis of high viscosity in concentrated antibody solutions: Strategies for high concentration drug product development, jan 2016. ISSN 19420870.

[17] Brian D Connolly, Chris Petry, Sandeep Yadav, Barthélemy Demeule, Natalie Ciaccio, Jamie M.R. Moore, Steven J Shire, and Yatin R Gokarn. Weak interactions govern the viscosity of concentrated antibody solutions: High-throughput analysis using the diffusion interaction parameter. *Biophysical Journal*, 103(1):69–78, 2012. ISSN 00063495. doi: 10.1016/j.bpj.2012.04.047.

[18] Barton J Dear, Jessica J Hung, Thomas M Truskett, and Keith P Johnston. Contrasting the Influence of Cationic Amino Acids on the Viscosity and Stability of a Highly Concentrated Monoclonal Antibody. *Pharmaceutical Research*, 34(1):193–207, 2017. ISSN 1573904X. doi: 10.1007/s11095-016-2055-5.

[19] Martin S. Neergaard, Devendra S. Kalonia, Henrik Parshad, Anders D. Nielsen, Eva H. Møller, and Marco Van De Weert. Viscosity of high concentration protein formulations of monoclonal antibodies of the IgG1 and IgG4 subclass - Prediction of viscosity through protein-protein interaction measurements. *European Journal of Pharmaceutical Sciences*, 49(3):400–410, 2013. ISSN 09280987. doi: 10.1016/j.ejps.2013.04.019.

[20] Shuntaro Saito, Jun Hasegawa, Naoki Kobayashi, Naoyuki Kishi, Susumu Uchiyama, and Kiichi Fukui. Behavior of Monoclonal Antibodies: Relation Between the Second Virial Coefficient (B 2) at Low Concentrations and Aggregation Propensity and Viscosity at High Concentrations. *Pharmaceutical Research*, 29(2 LB - Saito2012):397–410, 2012. ISSN 1573-904X. doi: 10.1007/s11095-011-0563-x.

[21] Priyanka Singh, Aisling Roche, Christopher F. van der Walle, Shahid Uddin, Jiali Du, Jim Warwicker, Alain Pluen, and Robin Curtis. Determination of Protein–Protein Interactions in a Mixture of Two Monoclonal Antibodies. *Molecular Pharmaceutics*, 16(12):4775–4786, dec 2019. ISSN 1543-8384. doi: 10.1021/acs.molpharmaceut.9b00430.

[22] P. Douglas Godfrin, Isidro E. Zarraga, Jonathan Zarzar, Lionel Porcar, Peter Falus, Norman J. Wagner, and Yun Liu. Effect of Hierarchical Cluster Formation on the Viscosity of Concentrated Monoclonal Antibody Formulations Studied by Neutron Scattering. *Journal of Physical Chemistry B*, 120(2):278–291, jan 2016. ISSN 15205207. doi: 10.1021/acs.jpcb.5b07260.

[23] Patrick M. Buck, Anuj Chaudhri, Sandeep Kumar, and Satish K. Singh.

Highly viscous antibody solutions are a consequence of network formation caused by domain-domain electrostatic complementarities: Insights from coarse-grained simulations. *Molecular Pharmaceutics*, 12:127–139, 1 2015. ISSN 15438392. doi: 10.1021/mp500485w.

[24] Anuj Chaudhri, Isidro E Zarraga, Tim J Kamerzell, J Paul Brandt, Thomas W Patapoff, Steven J Shire, and Gregory A Voth. Coarse-grained modeling of the self-association of therapeutic monoclonal antibodies. *J. Phys. Chem. B*, 116:8045–8057, 2012. doi: 10.1021/jp301140u. URL `https://pubs.acs.org/doi/pdf/10.1021/jp301140u`.

[25] Eric J. Yearley, Isidro E. Zarraga, Steven J. Shire, Thomas M. Scherer, Yatin Gokarn, Norman J. Wagner, and Yun Liu. Small-angle neutron scattering characterization of monoclonal antibody conformations and interactions at high concentrations. *Biophysical Journal*, 105(3):720–731, aug 2013. ISSN 00063495. doi: 10.1016/j.bpj.2013.06.043.

[26] Wayne G Lilyestrom, Sandeep Yadav, Steven J Shire, and Thomas M Scherer. Monoclonal antibody self-association, cluster formation, and rheology at high concentrations. *Journal of Physical Chemistry B*, 117 (21):6373–6384, 2013. ISSN 15205207. doi: 10.1021/jp4008152.

[27] Barton J. Dear, Jessica J. Hung, Joshua R. Laber, Logan R. Wilks, Ayush Sharma, Thomas M. Truskett, and Keith P. Johnston. Enhancing Stability and Reducing Viscosity of a Monoclonal Antibody With Cosolutes by Weakening Protein-Protein Interactions. *Journal of Pharmaceutical Sciences*, 108(8):2517–2526, mar 2019. ISSN 15206017. doi: 10.1016/j.xphs.2019.03.008.

[28] Miha Kastelic, Ken A. Dill, Yura V. Kalyuzhnyi, and Vojko Vlachy. Controlling the viscosities of antibody solutions through control of their binding sites. *Journal of Molecular Liquids*, 270:234–242, nov 2018. ISSN 01677322. doi: 10.1016/j.molliq.2017.11.106.

[29] Mahlet A. Woldeyes, Wei Qi, Vladimir I. Razinkov, Eric M. Furst, and Christopher J. Roberts. How Well Do Low- and High-Concentration Protein Interactions Predict Solution Viscosities of Monoclonal Antibodies? *Journal of Pharmaceutical Sciences*, 108(1):142–154, jul 2019. ISSN 15206017. doi: 10.1016/j.xphs.2018.07.007.

[30] Nicholas Skar-Gislinge, Michela Ronti, Tommy Garting, Christian Rischel, Peter Schurtenberger, Emanuela Zaccarelli, and Anna Stradner. A Colloid Approach to Self-Assembling Antibodies. *Molecular Pharmaceutics*, 16(6):2394–2404, jun 2019. ISSN 15438392. doi: 10.1021/acs.molpharmaceut.9b00019.

[31] William B. Russel. The Huggins coefficient as a means for characterizing suspended particles. *Journal of the Chemical Society, Faraday Transactions 2: Molecular and Chemical Physics*, 80(1):31–41, 1984. ISSN 03009238. doi: 10.1039/F29848000031.

[32] Karl F Freed and S F Edwards. Huggins coefficient for the viscosity of polymer solutions. *The Journal of Chemical Physics*, 62(10):4032–4035, 1975. ISSN 00219606. doi: 10.1063/1.430327.

[33] B. Cichocki and B. U. Felderhof. Diffusion coefficients and effective viscosity of suspensions of sticky hard spheres with hydrodynamic inter-

actions. *The Journal of Chemical Physics*, 93(6):4427–4432, 1990. ISSN 00219606. doi: 10.1063/1.459688.

[34] Johan Bergenholtz and Norman J. Wagner. The Huggins Coefficient for the Square-Well Colloidal Fluid. *Industrial & Engineering Chemistry Research*, 33(10):2391–2397, oct 1994. ISSN 0888-5885. doi: 10.1021/ie00034a021.

[35] Charles Tanford, John G Buzzell, David G Rands, and Sigurd A Swanson. The Reversible Expansion of Bovine Serum Albumin in Acid Solutions11. *Journal of the American Chemical Society*, 77(24):6421–6428, 1955. ISSN 15205126. doi: 10.1021/ja01629a003.

[36] Virgil L. Koenig and J. D. Perrings. Physicochemical effects of radiation. I. Effect of X-rays on fibrinogen as revealed by the ultracentrifuge and viscosity. *Archives of Biochemistry and Biophysics*, 38(1):105–119, 1952. ISSN 10960384. doi: 10.1016/0003-9861(52)90014-3.

[37] Donald E. McMillan. A comparison of five methods for obtaining the intrinsic viscosity of bovine serum albumin. *Biopolymers*, 13(7):1367–1376, 1974. ISSN 10970282. doi: 10.1002/bip.1974.360130708.

[38] K. Monkos. Viscosity of bovine serum albumin aqueous solutions as a function of temperature and concentration. *International Journal of Biological Macromolecules*, 18(1-2):61–68, 1996. ISSN 01418130. doi: 10.1016/0141-8130(95)01057-2.

[39] Karol Monkos. On the hydrodynamics and temperature dependence of the solution conformation of human serum albumin from viscometry

approach. *Biochimica et Biophysica Acta - Proteins and Proteomics*, 1700 (1):27–34, jul 2004. ISSN 15709639. doi: 10.1016/j.bbapap.2004.03.006.

[40] Karol Monkos. Determination of Some Hydrodynamic Parameters of Ovine Serum Albumin Solutions Using Viscometric Measurements. *Journal of Biological Physics*, 31:219–232, 2005. doi: 10.1007/s10867-005-1830-z.

[41] Jai A. Pathak, Sean Nugent, Michael Bender, Christopher J. Roberts, Robin J. Curtis, and Jack F. Douglas. Comparison of huggins coefficients and osmotic second virial coefficients of buffered solutions of monoclonal antibodies. *Polymers*, 13:1–21, 2 2021. ISSN 20734360. doi: 10.3390/polym13040601.

[42] Park M. Reilly, B. M.E. Van Der Hoff, and M. Ziogas. Statistical study of the application of the huggins equation to measure intrinsic viscosity. *Journal of Applied Polymer Science*, 24(10):2087–2100, nov 1979. ISSN 10974628. doi: 10.1002/app.1979.070241002.

[43] Ramón Pamies, José Ginés Hernández Cifre, María del Carmen López Martínez, and José García de la Torre. Determination of intrinsic viscosities of macromolecules and nanoparticles. Comparison of single-point and dilution procedures. *Colloid and Polymer Science*, 286(11):1223–1231, 2008. ISSN 0303402X. doi: 10.1007/s00396-008-1902-2.

[44] Rolando Curvale, Martin Masuelli, and Antonio Perez Padilla. Intrinsic viscosity of bovine serum albumin conformers. *International Journal of*

Biological Macromolecules, 42(2):133–137, 2008. ISSN 01418130. doi: 10.1016/j.ijbiomac.2007.10.007.

[45] Lorenzo Gentiluomo, Hristo L. Svilenov, Dillen Augustijn, Inas El Bialy, Maria Laura Greco, Alina Kulakova, Sowmya Indrakumar, Sujata Mahapatra, Marcello Martinez Morales, Christin Pohl, Aisling Roche, Andreas Tosstorff, Robin Curtis, Jeremy P. Derrick, Allan Nørgaard, Tarik A. Khan, Günther H.J. Peters, Alain Pluen, Åsmund Rinnan, Werner W. Streicher, Christopher F. Van Der Walle, Shahid Uddin, Gerhard Winter, Dierk Roessner, Pernille Harris, and Wolfgang Frieß. Advancing Therapeutic Protein Discovery and Development through Comprehensive Computational and Biophysical Characterization. *Molecular Pharmaceutics*, 17(2):426–440, jan 2020. ISSN 15438392. doi: 10.1021/acs.molpharmaceut.9b00852.

[46] Lorenzo Gentiluomo, Dierk Roessner, and Wolfgang Frieß. Application of machine learning to predict monomer retention of therapeutic proteins after long term storage. *International Journal of Pharmaceutics*, 577: 119039, jan 2020. ISSN 18733476. doi: 10.1016/j.ijpharm.2020.119039.

[47] Lorenzo Gentiluomo, Vanessa Schneider, Dierk Roessner, and Wolfgang Frieß. Coupling Multi-Angle Light Scattering to Reverse-Phase Ultra-High-Pressure Chromatography (RP-UPLC-MALS) for the characterization monoclonal antibodies. *Scientific Reports*, 9(1), dec 2019. ISSN 20452322. doi: 10.1038/s41598-019-51233-6.

[48] Lorenzo Gentiluomo, Dierk Roessner, Dillen Augustijn, Hristo Svilenov, Alina Kulakova, Sujata Mahapatra, Gerhard Winter, Werner Streicher,

Åsmund Rinnan, Günther H.J. Peters, Pernille Harris, and Wolfgang Frieß. Application of interpretable artificial neural networks to early monoclonal antibodies development. *European Journal of Pharmaceutics and Biopharmaceutics*, 141:81–89, aug 2019. ISSN 18733441. doi: 10.1016/j.ejpb.2019.05.017.

[49] Matja Zalar, Hristo L. Svilenov, and Alexander P. Golovanov. Binding of excipients is a poor predictor for aggregation kinetics of biopharmaceutical proteins. *European Journal of Pharmaceutics and Biopharmaceutics*, 151:127–136, jun 2020. ISSN 18733441. doi: 10.1016/j.ejpb.2020.04.002.

[50] Hristo Svilenov, Lorenzo Gentiluomo, Wolfgang Friess, Dierk Roessner, and Gerhard Winter. A New Approach to Study the Physical Stability of Monoclonal Antibody Formulations—Dilution From a Denaturant. *Journal of Pharmaceutical Sciences*, 107(12):3007–3013, dec 2018. ISSN 0022-3549. doi: 10.1016/J.XPHS.2018.08.004.

[51] D Roberts, R Keeling, M Tracka, C F Van Der Walle, S Uddin, J Warwicker, and R Curtis. Specific ion and buffer effects on protein-protein interactions of a monoclonal antibody. *Molecular Pharmaceutics*, 12(1): 179–193, 2015. ISSN 15438392. doi: 10.1021/mp500533c.

[52] D Roberts, R Keeling, M Tracka, C F Van Der Walle, S Uddin, J Warwicker, and R Curtis. The role of electrostatics in protein-protein interactions of a monoclonal antibody. *Molecular Pharmaceutics*, 11(7): 2475–2489, 2014. ISSN 15438392. doi: 10.1021/mp5002334.

[53] Daniel Corbett, Max Hebditch, Rose Keeling, Peng Ke, Sofia Eki-

zoglou, Prasad Sarangapani, Jai Pathak, Christopher F. Van Der Walle, Shahid Uddin, Clair Baldock, Carlos Avendan, and Robin A. Curtis. Coarse-Grained Modeling of Antibodies from Small-Angle Scattering Profiles. *Journal of Physical Chemistry B*, 121(35):8276–8290, 2017. ISSN 15205207. doi: 10.1021/acs.jpcb.7b04621.

[54] Alfredo Lanzaro, Aisling Roche, Daniel Corbett, Peter Davis, Nicole Sibanda, Maryam Shah, Shahid Uddin, Christopher F. van der Walle, Alain Pluen, and Robin A. Curtis. Role of Protein-Protein Interactions in Viscosity Enhancement and Non-Linear Rheometry of Concentrated Dispersions of Monoclonal Antibodies. *In press*, 2021.

[55] M. Shah, D. Corbett, A. Lanzaro, A. Roche, N. Sibanda, P. Davis, S. Uddin, C. F. van der Walle, R. Curtis, and A. Pluen. Micro- and macro-viscosity relations in high concentration antibody solutions. *European Journal of Pharmaceutics and Biopharmaceutics*, 153:211–221, jun 2020. ISSN 18733441. doi: 10.1016/j.ejpb.2020.06.007.

[56] Wyatt Technology. *ViscoStar III User ' s Guide*. Santa Barbara, USA, m1610 rev. edition, 2016.

[57] Mariya A. Pindrus, Steven J. Shire, Sandeep Yadav, and Devendra S. Kalonia. Challenges in Determining Intrinsic Viscosity Under Low Ionic Strength Solution Conditions. *Pharmaceutical Research*, 34(4):836–846, apr 2017. ISSN 1573904X. doi: 10.1007/s11095-017-2112-8.

[58] P. A. Charlwood. Sedimentation and Viscosity Studies in Bovine Serum

Albumin in Urea Solution. *Canadian Journal of Chemistry*, 33(6):1043–1054, jun 1955. ISSN 0008-4042. doi: 10.1139/v55-120.

[59] Pernille Sønderby, Jens T. Bukrinski, Max Hebditch, Günther H.J. Peters, Robin A. Curtis, and Pernille Harris. Self-Interaction of Human Serum Albumin: A Formulation Perspective. *ACS Omega*, 3(11):16105–16117, nov 2018. ISSN 24701343. doi: 10.1021/acsomega.8b02245.

[60] Marco Heinen, Fabio Zanini, Felix Roosen-Runge, Diana Fedunová, Fajun Zhang, Marcus Hennig, Tilo Seydel, Ralf Schweins, Michael Sztucki, Marián Antalík, Frank Schreiber, and Gerhard Nägele. Viscosity and diffusion: Crowding and salt effects in protein solutions. *Soft Matter*, 8 (5):1404–1419, feb 2012. ISSN 1744683X. doi: 10.1039/c1sm06242e.

[61] Jessica J. Hung, Wade F. Zeno, Amjad A. Chowdhury, Barton J. Dear, Kishan Ramachandran, Maria P. Nieto, Tony Y. Shay, Carl A. Karouta, Carl C. Hayden, Jason K. Cheung, Thomas M. Truskett, Jeanne C. Stachowiak, and Keith P. Johnston. Self-diffusion of a highly concentrated monoclonal antibody by fluorescence correlation spectroscopy: insight into protein–protein interactions and self-association. *Soft Matter*, 15 (33):6660–6676, 2019. ISSN 1744-683X. doi: 10.1039/C9SM01071H.

[62] Sonoko Kanai, Jun Liu, Thomas W. Patapoff, and Steven J. Shire. Reversible self-association of a concentrated monoclonal antibody solution mediated by fab-fab interaction that impacts solution viscosity. *Journal of Pharmaceutical Sciences*, 97(10):4219–4227, 2008. ISSN 15206017. doi: 10.1002/jps.21322.

[63] Sandeep Yadav, Steven J. Shire, and Devendra S. Kalonia. Viscosity behavior of high-concentration monoclonal antibody solutions: Correlation with interaction parameter and electroviscous effects. *Journal of Pharmaceutical Sciences*, 101(3):998–1011, mar 2012. ISSN 15206017. doi: 10.1002/jps.22831.

[64] Jayant Arora, Yue Hu, Reza Esfandiary, Hasige A Sathish, Steven M Bishop, Sangeeta B Joshi, C Russell Middaugh, David B Volkin, and David D Weis. Charge-mediated Fab-Fc interactions in an IgG1 antibody induce reversible self-association, cluster formation, and elevated viscosity. *mAbs*, 8(8):1561–1574, 2016. ISSN 19420870. doi: 10.1080/19420862.2016.1222342.

[65] Jozef Bicerano, Jack F. Douglas, and Douglas A. Brune. Model for the viscosity of particle dispersions. *Journal of Macromolecular Science - Reviews in Macromolecular Chemistry and Physics*, 39 C(4):561–642, 1999. ISSN 07366574. doi: 10.1081/mc-100101428.

[66] Lakshmi-narasimhan Krishnamurthy and Norman J. Wagner. The influence of weak attractive forces on the microstructure and rheology of colloidal dispersions. *Journal of Rheology*, 49(2):475–499, mar 2005. ISSN 0148-6055. doi: 10.1122/1.1859792.

[67] Matthias Roos, Maria Ott, Marius Hofmann, Susanne Link, Ernst Rössler, Jochen Balbach, Alexey Krushelnitsky, and Kay Saalwächter. Coupling and Decoupling of Rotational and Translational Diffusion of Proteins under Crowding Conditions. *Journal of the American Chem-*

ical Society, 138(32):10365–10372, aug 2016. ISSN 15205126. doi: 10.1021/jacs.6b06615.

[68] Derek E. Huang and Roseanna N. Zia. Sticky, active microrheology: Part 1. Linear-response. *Journal of Colloid and Interface Science*, 554: 580–591, oct 2019. ISSN 10957103. doi: 10.1016/j.jcis.2019.07.004.

[69] Eric J. Yearley, Paul D. Godfrin, Tatiana Perevozchikova, Hailiang Zhang, Peter Falus, Lionel Porcar, Michihiro Nagao, Joseph E. Curtis, Pradad Gawande, Rosalynn Taing, Isidro E. Zarraga, Norman J. Wagner, and Yun Liu. Observation of Small Cluster Formation in Concentrated Monoclonal Antibody Solutions and Its Implications to Solution Viscosity. *Biophysical Journal*, 106(8):1763–1770, apr 2014. ISSN 0006-3495. doi: 10.1016/J.BPJ.2014.02.036.

[70] Jun Liu, Mary D.H. Nguyen, James D. Andya, and Steven J. Shire. Reversible Self-Association Increases the Viscosity of a Concentrated Monoclonal Antibody in Aqueous Solution. *Journal of Pharmaceutical Sciences*, 94(9):1928–1940, sep 2005. ISSN 00223549. doi: 10.1002/jps.20347.

[71] Li Li, Sandeep Kumar, Patrick M. Buck, Christopher Burns, Janelle Lavoie, Satish K. Singh, Nicholas W. Warne, Pilarin Nichols, Nicholas Luksha, and Davin Boardman. Concentration dependent viscosity of monoclonal antibody solutions: Explaining experimental behavior in terms of molecular properties. *Pharmaceutical Research*, 31:3161–3178, 6 2014. ISSN 1573904X. doi: 10.1007/s11095-014-1409-0. URL `https://link.springer.com/article/10.1007/s11095-014-1409-0`.

[72] Elaheh Binabaji, Junfen Ma, and Andrew L Zydney. Intermolecular interactions and the viscosity of highly concentrated monoclonal antibody solutions. *Pharmaceutical Research*, 32:3102–3109, 9 2015. ISSN 1573904X. doi: 10.1007/s11095-015-1690-6. URL `http://link.springer.com/10.1007/s11095-015-1690-6`.

[73] Mariya A Pindrus, Steven J Shire, Sandeep Yadav, and Devendra S Kalonia. The effect of low ionic strength on diffusion and viscosity of monoclonal antibodies. *Molecular Pharmaceutics*, 15:3133–3142, 2018. ISSN 15438392. doi: 10.1021/acs.molpharmaceut.8b00210. URL `https://pubs.acs.org/sharingguidelines`.

[74] P Douglas Godfrin, Steven D Hudson, Kunlun Hong, Lionel Porcar, Peter Falus, Norman J Wagner, and Yun Liu. Short-Time Glassy Dynamics in Viscous Protein Solutions with Competing Interactions. *Physical Review Letters*, 115(22), 2015. ISSN 10797114. doi: 10.1103/PhysRevLett.115.228302.

[75] Vishnu L. Dharmaraj, P. Douglas Godfrin, Yun Liu, and Steven D. Hudson. Rheology of clustering protein solutions. *Biomicrofluidics*, 10 (4):043509, jul 2016. ISSN 1932-1058. doi: 10.1063/1.4955162.

[76] Ravi Chari, Kavita Jerath, Advait V. Badkar, and Devendra S. Kalonia. Long- and short-range electrostatic interactions affect the rheology of highly concentrated antibody solutions. *Pharmaceutical Research*, 26(12): 2607–2618, dec 2009. ISSN 07248741. doi: 10.1007/s11095-009-9975-2.

[77] Charles Tanford and John G. Buzzell. The viscosity of aqueous solutions

of bovine serum albumin between ph 4.3 and 10.5. *Journal of Physical Chemistry*, 60:225–231, 1956. ISSN 00223654. doi: 10.1021/j150536a020. URL `https://pubs.acs.org/sharingguidelines`.

[78] Prasad S. Sarangapani, Steven D. Hudson, Ronald L. Jones, Jack F. Douglas, and Jai A. Pathak. Critical examination of the colloidal particle model of globular proteins. *Biophysical Journal*, 108(3):724–737, feb 2015. ISSN 15420086. doi: 10.1016/j.bpj.2014.11.3483.

[79] Vivek Sharma, Aditya Jaishankar, Ying Chih Wang, and Gareth H. McKinley. Rheology of globular proteins: Apparent yield stress, high shear rate viscosity and interfacial viscoelasticity of bovine serum albumin solutions. *Soft Matter*, 7(11):5150–5160, jun 2011. ISSN 1744683X. doi: 10.1039/c0sm01312a.

[80] E. L. Hess and A. Cobure. The intrinsic viscosity of mixed protein systems, including studies of plasma and serum. *The Journal of general physiology*, 33(5):511–523, 1950. ISSN 00221295. doi: 10.1085/jgp.33.5.511.

[81] M. Y. Khan. Direct evidence for the involvement of domain III in the N-F transition of bovine serum albumin. *Biochemical Journal*, 236(1):307–310, 1986. ISSN 02646021. doi: 10.1042/bj2360307.

[82] Jinkee Lee and Anubhav Tripathi. Intrinsic viscosity of polymers and biopolymers measured by microchip. *Analytical Chemistry*, 77(22):7137–7147, nov 2005. ISSN 00032700. doi: 10.1021/ac050932r.

[83] Martin Masuelli and Denis Renard. *Advances in Physicochemical Properties of Biopolymers (Part 2)*. BENTHAM SCIENCE PUBLISHERS, aug 2017. ISBN 9781681085449. doi: 10.2174/9781681085449170101.

[84] J L Oncley, G Scatchard, and A Brown. Physical-chemical characteristics of certain of the proteins of normal human plasma. *Journal of Physical and Colloid Chemistry*, 51(1):184–198, 1947. ISSN 00223654. doi: 10.1021/j150451a014.

[85] George I Loeb and Harold A Scheraga. HYDRODYNAMIC AND THERMODYNAMIC PROPERTIES OF BOVINE SERUM ALBUMIN AT LOW pH1. *J. Am. Chem. Soc*, 13(8):829, 1956.

[86] John G. Buzzell and Charles Tanford. The effect of charge and ionic strength on the viscosity of ribonuclease. *Journal of Physical Chemistry*, 60(9):1204–1207, 1956. ISSN 00223654. doi: 10.1021/j150543a014.

[87] P. Johnson and A. J. Rowe. The intrinsic viscosity of myosin and the interpretation of its hydrodynamic properties. *The Biochemical journal*, 79:524–530, 1961. ISSN 02646021. doi: 10.1042/bj0790524.

[88] Jen Tsi Yang and Joseph F Foster. Intrinsic Viscosity and Optical Rotation of Proteins in Acid Media. *Journal of the American Chemical Society*, 77(9):2374–2378, 1955. ISSN 15205126. doi: 10.1021/ja01614a005.

[89] Max Hebditch, M. Alejandro Carballo-Amador, Spyros Charonis, Robin Curtis, and Jim Warwicker. Protein-Sol: A web tool for predicting protein solubility from sequence. *Bioinformatics*, 33(19):3098–3100, oct 2017. ISSN 14602059. doi: 10.1093/bioinformatics/btx345.

[90] Richard W. Mcdonogh and Robert J. Hunter. The Primary Electroviscous Effect. *Journal of Rheology*, 27(3):189–199, jun 1983. ISSN 0148-6055. doi: 10.1122/1.549704.

[91] F. S. Chan, J. Blachford, and D. A.I. Goring. The secondary electroviscous effect in a charged spherical colloid. *Journal of Colloid And Interface Science*, 22(4):378–385, 1966. ISSN 00219797. doi: 10.1016/0021-9797(66)90018-X.

[92] Stephen E. Harding. The intrinsic viscosity of biological macromolecules. Progress in measurement, interpretation and application to structure in dilute solution. *Progress in Biophysics and Molecular Biology*, 68(2-3): 207–262, sep 1997. ISSN 00796107. doi: 10.1016/S0079-6107(97)00027-8.

[93] Atul Saluja, Advait V Badkar, David L Zeng, Sandeep Nema, and Devendra S Kalonia. Application of high-frequency rheology measurements for analyzing protein–protein interactions in high protein concentration solutions using a model monoclonal antibody (IgG2). *Journal of Pharmaceutical Sciences*, 95(9):1967–1983, 2006. ISSN 1520-6017. doi: 10.1002/jps.20663.

[94] Ashlesha S. Raut and Devendra S. Kalonia. Viscosity Analysis of Dual Variable Domain Immunoglobulin Protein Solutions: Role of Size, Electroviscous Effect and Protein-Protein Interactions. *Pharmaceutical Research*, 33(1):155–166, jan 2016. ISSN 1573904X. doi: 10.1007/s11095-015-1772-5.

[95] Christian Lehermayr, Hanns-Christian Mahler, Karsten Mäder, and Ste-

fan Fischer. Assessment of Net Charge and Protein–Protein Interactions of Different Monoclonal Antibodies. *Journal of Pharmaceutical Sciences*, 100(7):2551–2562, jul 2011. ISSN 0022-3549. doi: 10.1002/JPS.22506.

[96] Richard W. O'Brien and Lee R. White. Electrophoretic mobility of a spherical colloidal particle, jan 1978. ISSN 03009238.

[97] Ian G. Watterson and Lee R. White. Primary electroviscous effect in suspensions of charged spherical particles. *Journal of the Chemical Society, Faraday Transactions 2: Molecular and Chemical Physics*, 77 (7):1115–1128, 1981. ISSN 03009238. doi: 10.1039/F29817701115.

[98] Hiroyuki Ohshima. A Simple Expression for Henry's Function for the Retardation Effect in Electrophoresis of Spherical Colloidal Particles. *Journal of Colloid and Interface Science*, 168(1):269–271, nov 1994. ISSN 0021-9797. doi: 10.1006/JCIS.1994.1419.

[99] A Einstein. Berichtigung zu meiner Arbeit: „Eine neue Bestimmung der Moleküldimensionen". *Annalen der Physik*, 339(3):591–592, jan 1911. ISSN 15213889. doi: 10.1002/andp.19113390313.

9. Supplementary Information

9.1. Published values for the intrinsic viscosity and Huggins coefficient of BSA in Literature

Reference	pH	Ionic Strength (mM)	T °C	$[\eta]$ ($mL\,g^{-1}$)	k_h	Max conc. ($mg\,mL^{-1}$)
Tanford (1956)[77]	7.3	10	25	4.12	2.88	40
Tanford (1956)[77]	7.3	100	25	3.65	2.1	40
Tanford (1956)[77]	7.3	500	25	3.71	1.96	40
Charlwood(1955)[58]	7	200	25.1	4.2	N/A	15
Sarangapani(2015)[78]	7.4	20	25	3.37	N/A	12
Sharma (2011)[79]	7.4	10	25	4	N/A	250
Curvale (2008)[44]	7.4	0	25	4.86	1.579	20
Hess (1950)[80]	7.4	100	37	4.2	N/A	20
Khan (1986)[81]	7	60	25	3.13	N/A	N/A
Pindrus(2017)[57]	7	200	25	3.6	N/A	1
Lee (2005)[82]	6.7-7.3	0	23	3.6	0.22	80
Masuelli (2017)[83]	6.5	Not Stated	25	4.57	10.24	4

Table 3: Collection of published values for the Intrinsic Viscosity and Huggins Coefficient of Bovine Serum Albumin in pH 7 conditions

Reference	pH	Ionic Strength (mM)	T °C	$[\eta]$ ($mL\,g^{-1}$)	k_h	Max conc. ($mg\,mL^{-1}$)
Koenig (1952)[36]	likely pH 5.2	200	25	4.18	1.33	300
Monkos (1996)[38]	5.2	0	25	5.8	0.745	363.4
Oncley (1947)[84]	likely pH 5.2	150	37	4.2	N/A	25
McMillan (1974)[37]	likely pH 5.2	150	37	4.07	1.369	90
McMillan (1974)[37]	likely pH 5.2	150	37	4.09	1.088	90
Loeb (1956)[85]	5.13	500	25	4.13	N/A	45
Sarangapani et al (2015)[78]	5	20	25	6.79	N/A	40
Tanford (1956)[77]	5	0	25	4.06	3.26	40
Tanford (1956)[77]	5	150	25	3.71	1.96	40

Table 4: Collection of published values for the Intrinsic Viscosity and Huggins Coefficient of Bovine Serum Albumin in pH 5 conditions. Where the pH is stated as "likely pH 5.2", the pH has not been explicitly stated or controlled by a named buffer but in the conditions provided the pH of the solution is likely at the isoelectronic point of BSA in low ionic strength, pH 5.2. The results in McMillan (1974)[37] are two measurements in the same conditions, measured two years apart and published in the same manuscript.

9.2. Intrinsic Viscosity is governed by electrostatic interactions

The intrinsic viscosity describes the contribution of the protein molecule to solution viscosity at infinite dilution. Intrinsic viscosity was a common parameter to measure in early studies to determine the conformation and hydrodynamic size of globular proteins[80,86,87,88]. The conformational expansion of BSA below pH 2.7 was discovered through observing the increase in intrinsic viscosity at these conditions[35]. The results of intrinsic viscosity measurements for PPI03 and PPI19 in a variety of formulations are presented in Figure 6. A pH dependence in the intrinsic viscosity data is observed at low ionic strength.

The isoelectric point, pI_{seq}, of PPI03 as calculated from the sequence using the Protein-Sol web server[89] (https://protein-sol.manchester.ac.uk/) is pH 9.4. The isoelectric point of PPI19 is pH 7.7. At low ionic strength, the further the pH of the solution from the pI, the higher the intrinsic viscosity for both PPI03 and PPI19. At a constant pH, a reduction in the intrinsic viscosity is observed when ionic strength is increased. This implicates electrostatic repulsion in the intrinsic viscosity changes in both PPI03 and PPI19 with variation in the formulation conditions. Further evidence that electrostatic repulsion plays a role in the intrinsic viscosity is shown in the similarity of the intrinsic viscosity values between the PPI03 pH 6.5 75 mM sample, the PPI03 pH 7.5 200 mM sample and the PPI03 pH 9 sample. The intrinsic viscosities for these samples are the lowest observed and are within the uncertainty of each other, despite having very different formulation conditions. The common factor in each of these three solutions is that the electrostatic repulsion is very low, either through screening by the high salt concentration or because

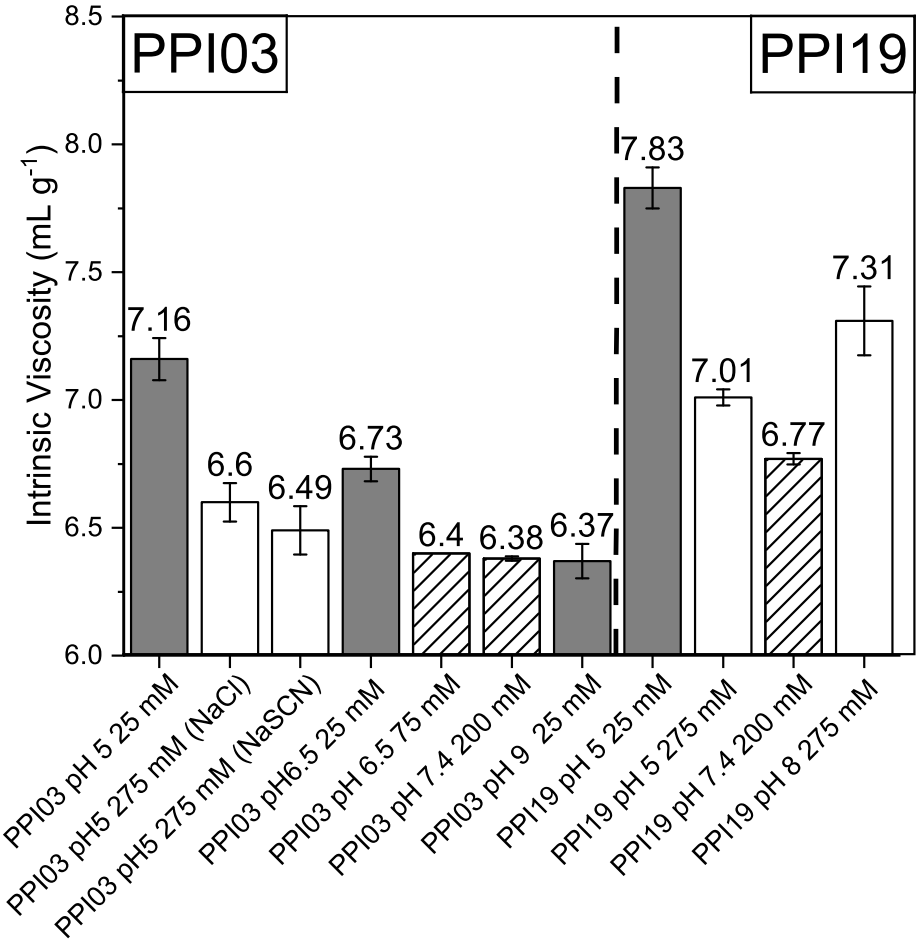

Figure 6: Intrinsic viscosity of PPI03 and PPI19 at a variety of pH and ionic strengths. The bars marked in black indicate measurements taken at 25 mM ionic strength . Patterned bars indicate measurements taken at intermiediate ionic strengths using a SEC-MALS-VISC set up, all others measured using MIDV.

the pH is close to the protein isoelectric point.

The effect of electrostatic interactions on solution viscosity has been described as three electroviscous effects. The primary electroviscous effect is the contribution to viscosity arising from the distortion of the ion cloud or double layer about the particle from the flow or movement of the molecule[90]. The secondary electroviscous effect is the result of overlapping electrostatic double layers as the molecules come within range of each other, with electrostatic range quantified by the Debye length[91], κ^{-1} . The tertiary electroviscous effect is rarely discussed in the context of proteins as it describes the contribution to viscosity from the effect of intramolecular electrostatics on polymer 'stiffness'[92]. The primary electroviscous effect is expected to be the most dominant effect of the three on the intrinsic viscosity as the measurement is taken at low protein concentrations, when the intermolecular distance is large[92].

Saluja et al.[93], Raut and Kalonia[94] and Pindrus et al.[57] found a pH dependence in the intrinsic viscosity of monoclonal antibodies, similar to our findings in Figure 6. Raut and Kalonia[94] and Pindrus[57] concluded that the intrinsic viscosity increase at lower pH values was due to either the primary electroviscous effect or changes in hydration of the molecule. Monoclonal antibodies have very low zeta potential for a colloidal molecule of their size[95,14,52] in the context of electroviscous theory[96,97]. It would be unusual for this marked change in intrinsic viscosity to be caused by such a low potential.

To interrogate the effect of the primary electroviscous effect on the intrinsic viscosity of the PPI03 solutions, the primary electroviscous coefficient, P_{E} was

calculated for each of the PPI03 25mM ionic strength conditions according to the equation set out by Watterson[97] using zeta potential measurements.

Zeta Potential measurements were carried out in triplicate using a Zetasizer Nano ZSP (Malvern, UK). Proteins were prepared by dialysis as described in the main Methods section, into 25mM NaCl solution with no buffer components added. Solutions were diluted to 1 mg ml^{-1} for analysis and titrated using 0.1M NaOH and 0.01M HCl. The voltage of the zeta potential measurements was 40V. A minimum of 15 runs were performed with a 60 second equilibration time prior to the measurement. The zeta potential was determined from the measured electrophoretic mobility by applying the Henry equation,

$$\mu_e = \frac{2\epsilon f(\kappa a)\zeta}{3\eta_0} \tag{11}$$

where μ_e is the electrophoretic mobility, ϵ is the dielectric constant of the medium, ζ is the zeta potential, and $f(\kappa a)$ is the Henry function calculated for each protein using the Ohshima[98] approximation and the R_h of the protein. The Henry function, $f(\kappa a)$, is approximately 1.1 for the antibodies in the conditions studied in this manuscript. The primary electroviscous effect is related to the bulk viscosity of a solution of charged spheres by the formula[97],

$$\eta_{rel} = 1 + 2.5\phi(1 + P_E(\frac{\zeta e}{k_b T}, \kappa a)) \tag{12}$$

where ϕ is the volume fraction of the solute and P_E is the primary electroviscous function e is electronic charge, k_b is the Boltzmann constant in units eV/T and T is temperature in units Kelvin.

The results of these calculations are shown in Table 5. The P_E term in the equation quantifies the amplification of the intrinsic viscosity as a result

of the primary electroviscous effect. P_{E} is a function proportional to both the magnitude of the reduced zeta potential, ζ_{red}, and the Debye length-particle radius ratio, κa. The P_{E} values in Table 5 are much too low to explain the pH-dependence in intrinsic viscosity shown in Figure 6.

pH	**Ionic strength**	ζ_{red}^{exp}	$\mathbf{P}_E^{exp}$
5	25	0.54	0.006
6.5	25	0.43	0.004
9	25	-0.05	0.0001

Table 5: Values calculated for the primary electroviscous effect coefficient P_E for samples of PPI03 at 25mM NaCl at varying pH levels. $\zeta_{\mathrm{red}}{}^{\mathrm{exp}}$ and $P_{\mathrm{E}}{}^{\mathrm{calc}}$ are based on an experimentally determined zeta potential values.

It's possible that the tertiary electroviscous effect could be a contributing factor in the pH-dependence of intrinsic viscosity at low ionic strength. The tertiary electroviscous effect discussed earlier is rarely considered for proteins as the tightly folded structure and globular form make it unlikely to be affected by intramolecular interactions. However, if the Fab and Fc subdomains of the molecule are similarly charged as is likely at pHs far from the pI, the domains of the protein will experience an electrostatic repulsion between each other. This would lead to the Fabs and Fc reorienting themselves to be as distant as possible from each other, extending the hinge as much as possible positively contributing to the intrinsic viscosity. Increasing the pH towards the pI would not only reduce the overall charge of the subunits, but also increase the surface charge heterogeneity, reducing the intraprotein repulsion and in turn reducing the intrinsic viscosity. The effect of ion binding at the

surface would also yield lower intraprotein repulsion, in line with the lower intrinsic viscosities observed at higher ionic strengths.

Protein	PPI03					PPI19		
Formulation	pH5 25 mM	pH5 275 mM NaCl	pH 5 275 mM NaSCN	pH 6.5 25 mM	pH 9 25 mM	pH5 25 mM	pH5 275 mM NaCl	pH8 250 mM NaCl
R_h,visc (nm)	5.47	5.32	5.29	5.35	5.26	5.69	5.49	5.56
R_h,visc (+/-)	0.008	0.008	0.011	0.001	0.004	0.006	0.005	0.019
% Monomer	99.3	98	N/A	99.3	98.7	94	94.5	91.7

Table 6: Hydrodynamic radius values calculated from the intrinsic viscosity results for PPI03 and PPI19 and monomer fraction results measured by SEC-MALS. There were no observable low molecular weight species peaks in the analyses. The PPI03 pH 5 275 mM NaSCN sample was not available for SEC-MALS measurement.

An estimate of the hydrodynamic radius, R_h, of the protein can be made from the intrinsic viscosity using the Einstein-Simha formula[99]:

$$R_h = \left[\frac{3[\eta]M_w}{10\pi N_a}\right]^{\frac{1}{3}} \tag{13}$$

where M_w is the molecular weight of the protein and N_a is Avogadro's constant. The R_h values calculated from the intrinsic viscosity results are tabulated in Table 6. These agree well with the hydrodynamic radius of between 5.0-5.3 nm reported for PPI03 in Roberts et al.[52] and the hydrodynamic radius for PPI19 of 5.6 nm at pH 5 low ionic strength and 5.35 nm at all high ionic strength conditions from the results presented in Singh et al.[21]. Since the intrinsic viscosity scales with the third power of the hydrodynamic radius, it is sensitive to even very small changes in protein hydrodynamic size, which

may not be detectable by orthogonal methods such as measuring diffusion coefficients by dynamic light scattering.

The intrinsic viscosity of a sample is also sensitive to the presence of oligomers in solution. The samples of PPI03 and PPI19 used in the MIDV analysis were subject to SEC-MALS analysis to ascertain the level of irreversible aggregation present, presented in Table 6. For PPI03, all samples had greater than 98% monomer and no pH effect was observed. The results for the PPI19 samples show there are some high molecular weight species in solution as the monomer fraction is slightly lower. The increase in the $[\eta]$ measured for the PPI19 pH 8 sample is against the general trend and is likely a result of a greater population of high molecular weight species in this sample. The monomer fraction is very similar between samples of the same protein despite large difference in intrinsic viscosity demonstrating that the effect of electrostatics is the more dominant influence on the intrinsic viscosity in these solutions.